PAPER • **OPEN ACCESS**

Antifungal activity of biosynthesized silver nanoparticles from *Candida albicans* on the strain lacking the *CNP*41 gene

To cite this article: Darshan Dhabalia *et al* 2020 *Mater. Res. Express* **7** 125401

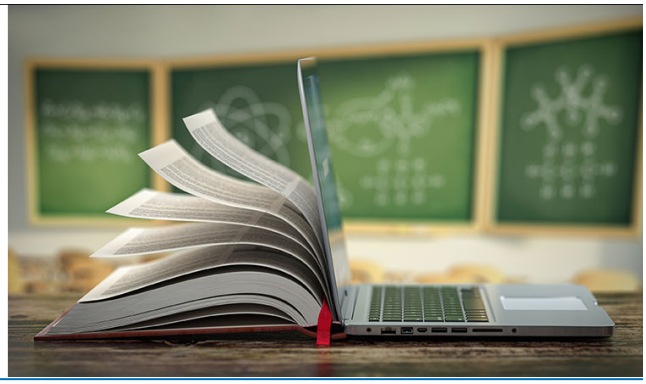

Materials Research Express

PAPER

Antifungal activity of biosynthesized silver nanoparticles from *Candida albicans* on the strain lacking the *CNP*41 gene

Darshan Dhabalia[1], **Shareefraza J Ukkund**[2,3], **Usman Taqui Syed**[4], **Wasim Uddin**[1] and **M Anaul Kabir**[1]

[1] Molecular Genetics Laboratory, School of Biotechnology, National Institute of Technology Calicut, Calicut, Kerala, 673601, India
[2] Department of Nano-Technology, Srinivas Institute of Technology, Mangalore, 574143, India
[3] Centre for Nanoscience & Technology, College of Engineering and Technology, Srinivas University, Mangalore, 574146, India
[4] LAQV/REQUIMTE, Laboratory of Membrane Processes, Department of Chemistry, Faculty of Science and Technology, Nova University of Lisbon, Campus de Caparica, 2829-516 Caparica, Portugal

E-mail: anaulk@nitc.ac.in

Keywords: *Candida albicans*, *CNP*41 gene, silver nanoparticles, drug susceptibility, fluconazole

OPEN ACCESS

RECEIVED
16 October 2020

REVISED
17 November 2020

ACCEPTED FOR PUBLICATION
20 November 2020

PUBLISHED
2 December 2020

Abstract

The upsurge of immunocompromised patients has led to extensive study of fungal infections with *Candida albicans* being the frontline model of pathogenic yeast in humans. In the quest to find novel antifungal agents, this study reports the potential usage of wild-type *C. albicans* strain C86 to biosynthesise silver nanoparticles by microwave assisted technique. Visual colour change and UV-spectrophotometer were used for primary detection of silver nanoparticles. Additionally, the FTIR peaks confirm the particles' formation and surface characterisation techniques such as FESEM and EDX suggests that the silver nanoparticles were sized in the range of 30–70 nm. Furthermore, pioneering work of homologous recombination technique was systematically employed to delete uncharacterized gene *orf*19.3120 (*CNP*41) in the C86 strain creating the deletion strain C403 of *C. albicans*. To amalgamate the two significant findings, biosynthesized silver nanoparticles were subjected to antifungal studies by disk diffusion assay on the strain C403 that lacks the gene *orf*19.3120 (*CNP*41) of *C. albicans*. As a synergetic approach, combinational effect was studied by incorporating antifungal drug fluconazole. Both individual and enhanced combinational antifungal effects of silver nanoparticles and fluconazole were observed on genetically modified C403 strain with 40% increase in fold area compared to wild-type C86 strain. This can be attributed to the synergetic effect of the bonding reaction between fluconazole and AgNPs. Taken together, this first-ever interdisciplinary study strongly suggests that the *CNP*41 gene could play a vital role in drug resistance in this fungal pathogen.

1. Introduction

Diverse populations of microbes like bacteria and fungi have advertently inhabited the human race with the passage of time. Although some of the microbial interactions have been beneficial, yet their detrimental effects are numerous. Of late, with increase in the number of immunocompromised patients, the study of fungal infections has gained more prominence in medical research with *Candida albicans* being one of the frontline model of pathogenic yeast in humans [1]. *C. albicans* is a diploid fungus, polymorphic in nature having the ability to grow as yeast, pseudohyphae and true hyphae [2, 3]. Several studies demonstrated that *C. albicans* is the most prevalent fungal pathogen that can cause multiple diseases ranging from superficial infections of mucous membranes to life-threatening systemic candidemia [1, 4].

In the last few decades, several antifungal drugs have been developed to treat *Candida* infections. Based on their chemical composition and mode of action, antifungals have been classified into different groups such as allylamines, azoles, echinocandins, 5-fluorocytosine and polyenes [5]. Among these groups, azole class of antifungals are preferred due to its broad spectrum activity, high efficacy and low toxicity. However, long-term

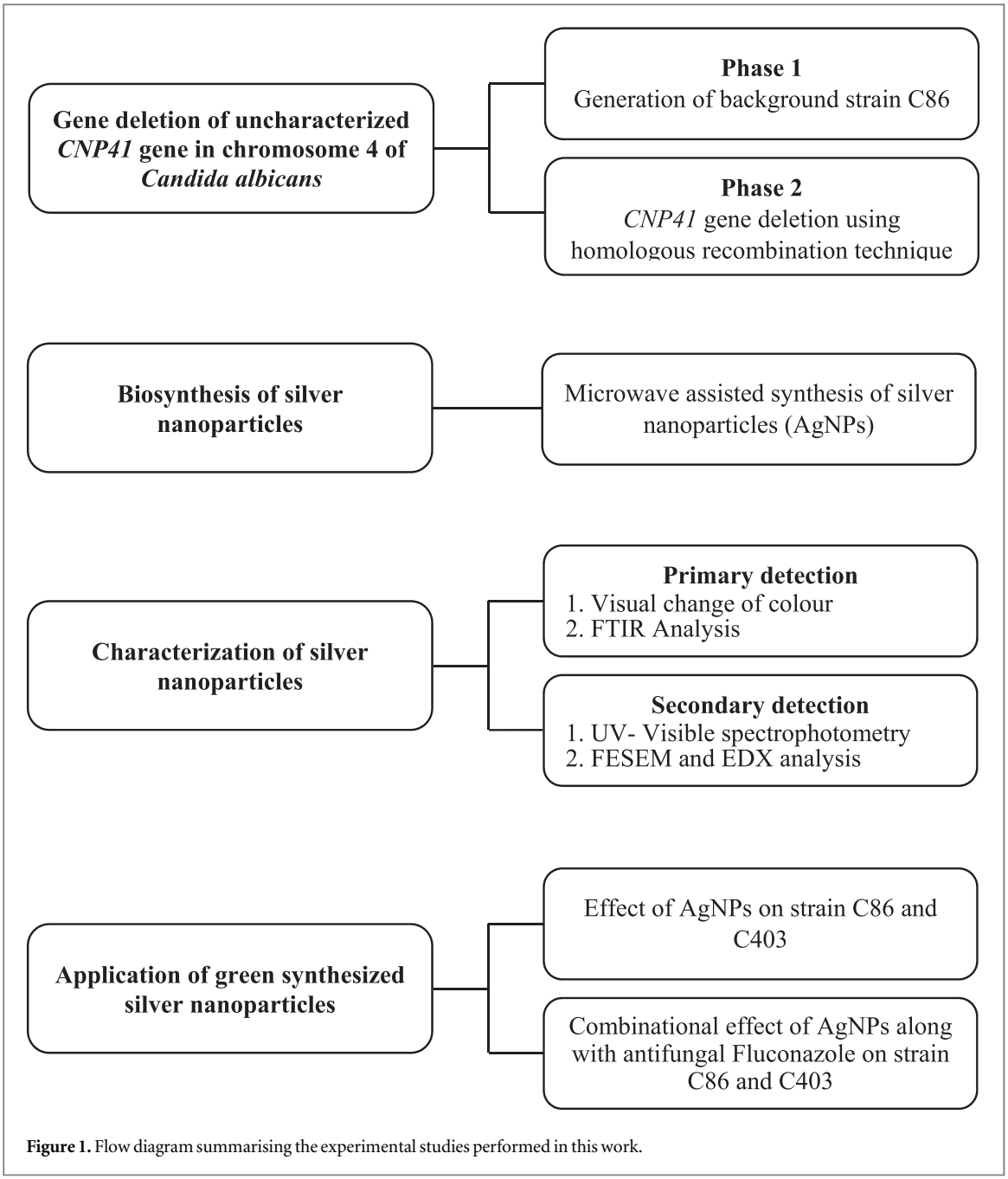

Figure 1. Flow diagram summarising the experimental studies performed in this work.

therapy or repeated use of these antifungals leads to the development of resistance among the *candida* species which could in turn affect the individuals having weak defence mechanisms [6]. To overcome the current challenges witnessed in the existing conventional antifungal agents, the present work addresses the dire need to explore a novel antifungal agent which would also be cost-effective with lesser side effects.

Several alternative strategies to produce antifungal agents include antifungal peptides, efflux pump inhibitors, essential oils, nanoparticles, oxidative stress markers, phytochemicals and statins to mention a few [7]. Among these, metal oxide nanoparticles have several advantages which include intracellular free radical generation, large surface to volume ratio, membrane damage, metal ion release and multiple cellular targets that can prevent the risk of resistance development [8]. Recent studies suggest that the importance of silver in the health care sector has driven research to shift from ionic or colloidal silver based usage to silver nanoparticles (AgNPs) as they have a better safety profile. Moreover, AgNPs have a broad spectrum of antibacterial, antifungal and antiviral activities [9, 10]. Nevertheless, the production of silver nanoparticles using physicochemical methods would be expensive, dangerous and toxic to human health and environment [11]. Therefore, biosynthesis of silver nanoparticles to combat the environmental hazards sets the premise of the current study.

In recent years, literature emphasises the biosynthesis approach for producing silver nanoparticles due to its simple, non-toxic, eco-friendly and cost-effective benefits. Moreover, it does not require any capping agents or

Table 1. List of strains.

Strains	Description	Phenotype	Source
CAF4-2	Wild-type strain	Ura^-	[15]
C86	*Δura3::imm434/Δura3::imm434 Δleu2::FRT/Δleu2::FRT*	$Ura^- Leu^-$	This study
C386	Single copy deletant of *CNP*41 gene	Ura^+	This study
C403	Double copies deletant of *CNP*41 gene	$Leu^+ Ura^+$	This study

surfactants which was required by physicochemical methods [12]. The mode of action of AgNPs using biosynthesis approach is yet to be explored in detail and sporadic distribution of literature is seen regarding the studies of antifungal properties of silver nanoparticles [10–13]. In the current study, novel work has been carried out to synthesise AgNPs from a wild-type *Candida* strain C86 using biosynthesis approach and microwave assisted technique. The formation of AgNPs was characterized by primary and secondary detection techniques. Primary detection of presence of silver nanoparticles included the observation of the colour change of the solution from pale yellow to brown, followed by FTIR analysis. Secondary detection was carried out by using a double beam UV Spectrophotometer and further confirmed by EDX and FESEM analysis.

From *Candida* Genome Database (CGD), it has been found that open reading frame (ORF)/gene *orf*19.3120 located on chromosome 4 on the right arm (chromosomal coordinates 1538056-1539795; ORF size 1740 bp) remains uncharacterized and it has been predicted to be a putative PDR-subfamily ABC transporter using bioinformatics approach [14]. This ORF/gene has been taken in this study as it lacks any experimental evidence to prove its role in *C. albicans* drug resistance arsenals. Moreover, it encodes a protein of half size of ABC transporters Cdr1p and Cdr2p. Therefore, we have attempted to investigate its role in drug resistance by novel approach using AgNPs. Otherwise its function could have been masked by other stronger ABC transporters encoded by the genes *CDR*1 and *CDR*2 and would not be amenable for functional analysis. The nanoparticles obtained were tested on the uncharacterized gene, *orf*19.3120 (designated as *CNP*41 gene). Both the copies of the *CNP*41 gene were deleted in the wild-type strain C86 generating the strain C403 (*cnp*41Δ/*cnp*41Δ). Antifungal activity of silver nanoparticles was tested on C403 strain using disk diffusion method. Nanoparticles alone and in combination with fluconazole were used in this study.

2. Materials and methods

2.1. Experimental procedure

The flowchart of the procedures has been presented in figure 1. Briefly, double copy deletion of *CNP*41 has been done in two phases, Phase I and Phase II. Biosynthesis of silver nanoparticles was followed by its primary and secondary detection and characterization. Lastly, these nanoparticles were tested on *CNP*41 deleted strain for their antifungal activity.

2.2. Strains

Candida albicans strain C86 (*Δura3::imm434/Δura3::imm434 Δleu2::FRT/Δleu2::FRT*) was derived from CAF4-2 (*Δura3::imm434/Δura3::imm434*) [15] by deleting both the copies of *LEU*2 gene using construct pKA76 [16] and evicting *URA*3 flipper as described by Morschhäuser *et al* [17]. The plasmid pKA76 was digested with *Kpn*I-*Sac*I to release the deletion cassette and transformed into parental strain CAF4-2 to delete both the copies of *LEU*2 gene and *URA*3 flipper was evicted by incubating in yeast carbon base (YCB) media in presence of bovine serum albumin as described by Morschhäuser *et al* [17]. The resulting strain C86 was used for deleting the gene *CNP*41 (*orf*19.3120). For routine amplification of plasmids and subcloning of DNA fragments, *Escherichia coli* strain XL-1 Blue was used [18]. Table 1 details the strains used in this study.

2.3. Media and growth condition

Yeast extract/peptone/dextrose (YPD) and synthetic dextrose (SD) media were prepared for culturing the yeast strain as described [19]. Uridine 50 μg ml^{-1} was supplemented additionally as per the requirement. Strains were maintained in 15% v/v glycerol stock and stored in −80 °C. *Candida albicans* strains were streaked freshly to avoid spontaneous chromosomal instability when required [20]. Bacterial strains were grown in yeast extract/tryptone/sodium chloride (YT) media (0.5% sodium chloride, 0.5% yeast extract and 1% tryptone) at 37 °C. Plasmids were amplified in YT media containing 100 μg ml^{-1} of ampicillin.

2.4. Molecular biology methods

PCR amplification was performed using a thermal cycler as described [21]. Restriction digestion of plasmids, gel elution of DNA fragments, ligation of DNA fragments into vectors were carried out as described [22]. Plasmids

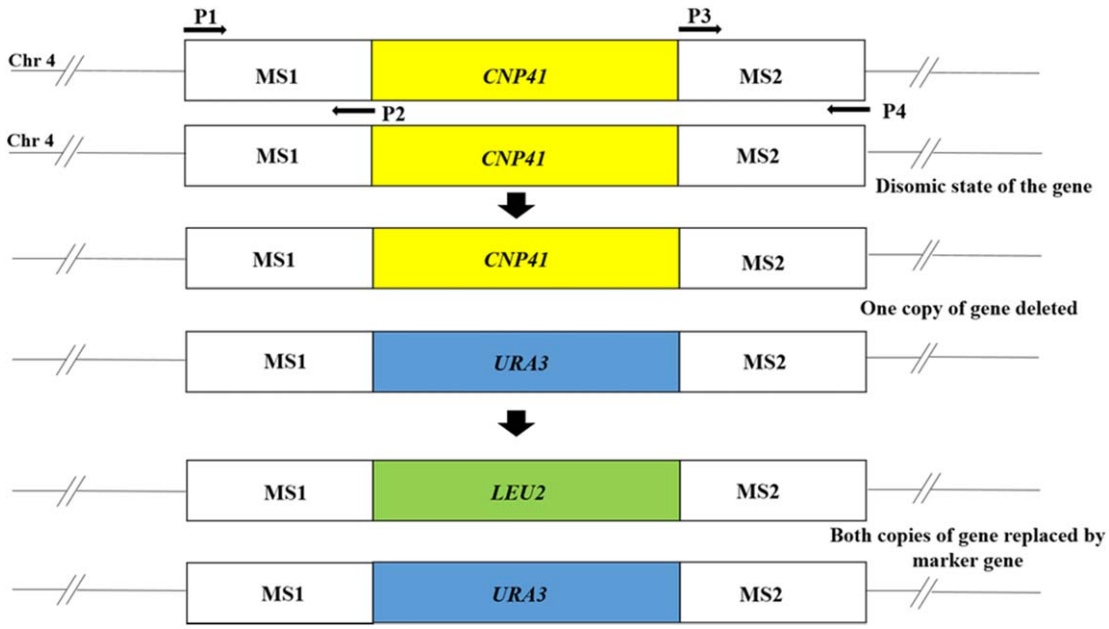

Figure 2. Schematic diagram of deletion of *CNP*41 gene located on chromosome 4. MS1 and MS2 are flanking sequences of *CNP*41 gene. MS1 was PCR amplified using primers P1 and P2; MS2 amplified using P3 and P4. *URA*3 and *LEU*2 are selection markers.

were isolated by alkaline lysis method [23]. *E. coli* transformation was carried out by calcium chloride method [24]. *C. albicans* transformation was done by spheroplast method [25, 26].

2.5. Vectors, plasmid constructs and primers

Plasmid pUC19 was used for cloning and sequencing purposes [27]. The plasmid pSFU1 containing *URA*3 flipper was provided by. Morschhäuser as a gift. The plasmid pKA16 was made by subcloning a 1.4 kb *Sal*I-*Pst*I fragment containing *URA*3 (digested out from pSFU1) into pUC19 at *Sal*I/*Pst*I site. The plasmid pKA16 was used as basic plasmid to make constructs for gene/ORF deletion. Primers used in this study are listed in table 2. Primers KC16, KC17 (*URA*3) and KC195, KC206 (*LEU*2) are made using internal sequences of selection markers [16].

The *LEU*2 deletion construct was made by subcloning flanking sequences of *LEU*2 gene into *URA*3 flipper plasmid pSFUI. Upstream and downstream sequences were amplified using the primers KC74/KC75 and KC76/KC77 from CAF4-2 genomic DNA. The PCR products were inserted into plasmid pSFUI at *Kpn*I/*Xho*I and *Sac*I/*Not*I sites generating pKA76. The plasmid pKA76 can be digested with *Kpn*I-*Sac*I to release the deletion cassette and transform into recipient *Candida* strain.

The *CNP*41 gene deletion was done as shown in figure 2. The *CNP*41 gene deletion construct was made by subcloning flanking sequences on either side of the selection marker. Briefly, two sets of primers, KC186/KC187 and KC188/KC189 (table 2) were made by using the *Candida albicans* genome sequence available at *Candida* Genome Database. PCR products of 525 bp and 505 bp were amplified using genomic DNA of parental strain CAF4-2. These PCR products were cloned into pTZ57R/T vector using InsTA PCR Cloning kit as recommended by the manufacturer (Thermo Fisher Scientific, Lithuania). Subsequently, these two products were digested out from pTZ57R/T and inserted at *Sac*I/*Bam*HI and *Pst*I/*Hind*III sites of pKA16 generating the plasmid pKA244 carrying *URA*3 marker for first copy deletion of *CNP*41 gene. Second deletion construct carrying the *LEU*2 marker was made by replacing *URA*3 with *LEU*2 (taken out from pKA188) gene in pKA244 resulting in the plasmid pKA594. The plasmid pKA244 was digested with *Sac*I/*Hind*III to release the deletion cassette and transformed into *Candida* strain C86 for deleting the first copy of the *CNP*41 gene. Subsequently, the second copy was deleted by transforming a single copy deleted strain with the plasmid pKA594. Plasmids used in this study are listed in table 3.

2.6. Confirmation strategy for gene deletion

Deletion of the *CNP*41 gene was confirmed by PCR with two pairs of primers for checking 5′ and 3′ junctions. Double deletions were verified with internal primers and the primers used for this purpose are listed in table 2. PCR products of 5′ and 3′ junctions were also digested with restriction enzymes to ensure that there are no non-specific amplifications.

Table 2. List of Primers used in the study.

Primer no.	Sequence (5′→3′)	Purpose
KC 74	TCGGGTACCGTTAGTTTCTATTATGGCCGTCAA	Amplification of 990 bp upstream of *LEU*2, will be used for deletion this *LEU*2 using *URA*3 flipper
KC 75	TCGCTCGAGGGATATTGGTTTTAAAAGAAAGGA	
KC 76	TCGGCGGCCGCCAGTAGTTAGCATTTAAATTTCAAATACT	Amplification of 988 bp downstream of *LEU*2, will be used for deletion this *LEU*2 using *URA*3 flipper
KC 77	TCGGAGCTCAATACGTTTATACCACGTGGTGAC	
KC 186	GAGCTCGAAGGCATCAAAGAAGGATTTG	Amplification of 525 bp upstream of orf19.3120, will be used for deleting *CNP*41 gene
KC 187	GGATCCGACTTATTTGCAATTATTGTTAAAATG	
KC 188	CTGCAGCTCGTACAGAAATGTACTCTTTACG	Amplification of 505 bp downstream of *orf*19.3120, will be used for deleting *CNP*41 gene
KC 189	AAGCTTCCCTGCTGCTGATAATCCTTAT	
KC 16	GTCTTGATTAAGCATACATAAGGAC	For verifying deletion of *orf*19.3120, using *URA*3 marker
KC 17	TGAAGTTGTTAGCACTGGAACTG	
KC 195	GATGATTTAGCACTTTCAAGAGC	For verifying deletion of *orf*19.3120, using *LEU*2 marker
KC 206	AGCGGTATCAGAACAGCAGA	
KC 192	CATGTGACTCAATGGTATAATGATG	For verifying deletion of upstream of *orf*19.3120, upstream on Chr4
KC 193	CAAACATGATTGTAGAAGAAGATC	For verifying deletion of upstream of *orf*19.3120, downstream on Chr4
KC 398	ATGGCTCTGTTAGTGCTGGAGAA	Internal primers of *CNP*41 gene to verify double copy deletion.
KC 399	TGTACGCAACTGACATAAACGAC	

Table 3. List of plasmids.

Plasmid Name	Description	References
pSFU1	Vector	[17]
pUC19	Vector	[27]
pKA16	*URA*3 marker cloned in pUC19	This study
pKA188	*LEU*2 marker cloned in pUC19	This study
pKA244	*CNP*41 gene deletion construct containing *URA*3 marker	This study
pKA594	*CNP*41 gene deletion construct containing *LEU*2 marker	This study
pKA76	*LEU*2 deletion construct	[16]

2.7. Biosynthesis of silver nanoparticles

Nanoparticles were synthesized using biosynthesis approach and microwave assisted technique using wild-type *C. albicans* strain C86. Procedure for nanoparticles biosynthesis has been briefly described herein. The *Candida* strain C86 stored in −80 °C ultra-freezer was streaked on YPD plate supplemented with uridine (50 μg ml^{-1}) and incubated at 30 °C for 12–16 h to get barely visible young colonies. The cells were then inoculated into a 100 ml YPD liquid supplemented with uridine (50 μg ml^{-1}). Cells were incubated at 30 °C in shaking incubator at 110 rpm for 16–18 h. The cells were filtered using Whatman grade 01 filter paper [28]. 100 ml silver nitrate solution was prepared using MilliQ water with its concentration (0.1 M). The resultant 50 ml of cell filtrate was taken and mixed with silver nitrate solution in 1:1 ratio [29]. The mixture was then heated at 600 W for 5 min till the mixture reduces Ag^{+} to Ag^{0} by changing its colour from pale yellow to brown [29].

2.8. Characterization of silver nanoparticles

The solution of prepared nanoparticles was subjected to double beam UV spectrophotometer (Systronics 2202, India) for primary confirmation of synthesis of AgNPs. The silver nanoparticles sample was tested along with control microbial suspension. As silver nanoparticles' range of wavelength falls under 400–480 nm, the range was set at 200–800 nm. Furthermore, the synthesised AgNPs were centrifuged to obtain pellets and then characterized by FTIR (JASCO V 600, Japan) for observing the functional groups. EDX and FESEM (Carl Zeiss sigma, Germany) techniques were incorporated to view size and shape of silver nanoparticles.

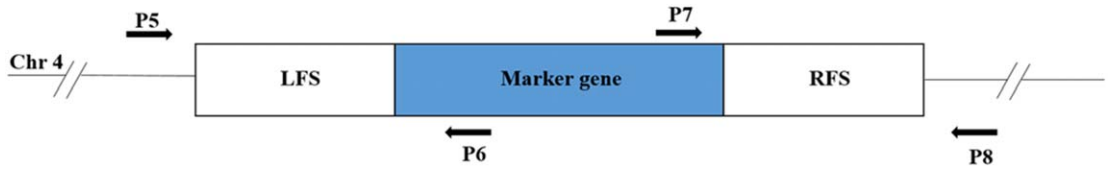

Figure 3. Schematic diagram of primer design for verifying the *CNP*41 gene deletion. Chr4, chromosome 4 of *C. albicans*; LFS and RFS, flanking sequences on the left side and right side of the gene used for making deletion constructs. Primers P5 and P8 are designed from chromosomal DNA sequence outside LFS and RFS whereas P6 and P7 are designed from selection marker which is used for deletion.

2.9. Antifungal susceptibility test

Disc diffusion test was performed to evaluate the antifungal activity as described [30]. Sterile 6 mm disks were purchased from Himedia, India. 20 μl of silver nanoparticles was pipetted onto the sterile disk. Standard disks of fluconazole (10 μg, Himedia) was used as positive control and combination of fluconazole with AgNPs was impregnated on the disks for this study. SD plates containing *Candida* cells and disk were incubated at 30 °C for 24–48 h until a clear zone of inhibition was formed. The diameter of these zones was measured. The protocol was followed as described [30]. Each test was conducted in triplicates to ensure reproducibility.

2.10. Assessment of increase in fold area

The increase in fold area was assessed by calculating the mean surface area of the zone of inhibition of antifungal activity of fluconazole alone and fluconazole along with AgNPs. The percentage fold increase in area of tested antifungal activity was calculated from equation (1):

$$\%\ fold\ increase\ in\ area\ of\ tested\ antifungal\ activity = \frac{B - A}{A} * 100 \quad (1)$$

where, A is the zone of inhibition of tested antifungal alone and B is the zone of inhibition of tested antifungal along with synthesized silver nanoparticle [31].

3. Results and discussion

3.1. Deletion of *CNP*41 gene in Candida albicans

The *Candida albicans* strain C86 was transformed with the plasmid pKA244 by digesting with *Sac*I/*Hind*III and ura$^+$ transformants were obtained on plate lacking uridine (ura$^-$ plate). The ura$^+$ transformants were re-streaked on the ura$^-$ plate to remove any false transformants. Transformants were independently processed for making genomic DNA for PCR verification of *CNP*41 gene deletion. PCR verification of the junctions was done as shown in figure 3. Both 5′ and 3′ junctions were verified by primers KC16/KC192 and KC17/KC193 respectively. The expected sizes of amplified products for 5′ and 3′ junction verification would be 811 bp and 901 bp, respectively. The obtained PCR products were exactly matching with the expected sizes (see figure 4(a). Further confirmation comes from the digestion of these PCR products with diagnostic restriction enzymes producing the fragments of expected size (data not shown). Approximately 15 ura$^+$ transformants were screened by this process and 3 right candidates were obtained for first copy deletion of *CNP*41 gene. Henceforth, we refer *orf*19.3120 as *CNP*41 (*Candida* Nanoparticle 41). The strain carrying the first copy deletion was designated as C386.

For the deletion of the second copy of the *CNP*41 gene, the strain C386 was transformed with the plasmid pKA594 and leu$^+$ transformants were obtained on the SD plate lacking leucine. The transformants were processed for genomic DNA preparation and subsequently PCR was done to screen the right candidates. The primers KC195/KC192 and KC206/KC193 were used for verifying 5′ and 3′ junctions. Expected size of the PCR products are 811 bp and 901 bp, respectively. The sizes of the PCR products obtained are matching with the expected sizes (see figure 4(b)). PCR products were further digested with diagnostic restriction enzymes to ensure that they are not non-specific bands (data not shown). Approximately 40 leu$^+$ transformants were screened and 8 right candidates were obtained. Deletion of *CNP*41 gene was further confirmed by designing a pair of internal deletion primers KC398/KC399 which would fail to amplify any product in the double copy deleted strain whereas parental strain would produce a band of 1035 bp (see figure 5). Thus, the *CNP*41 gene was successfully deleted, generating the strain C403 (*cnp*41Δ/*cnp*41Δ).

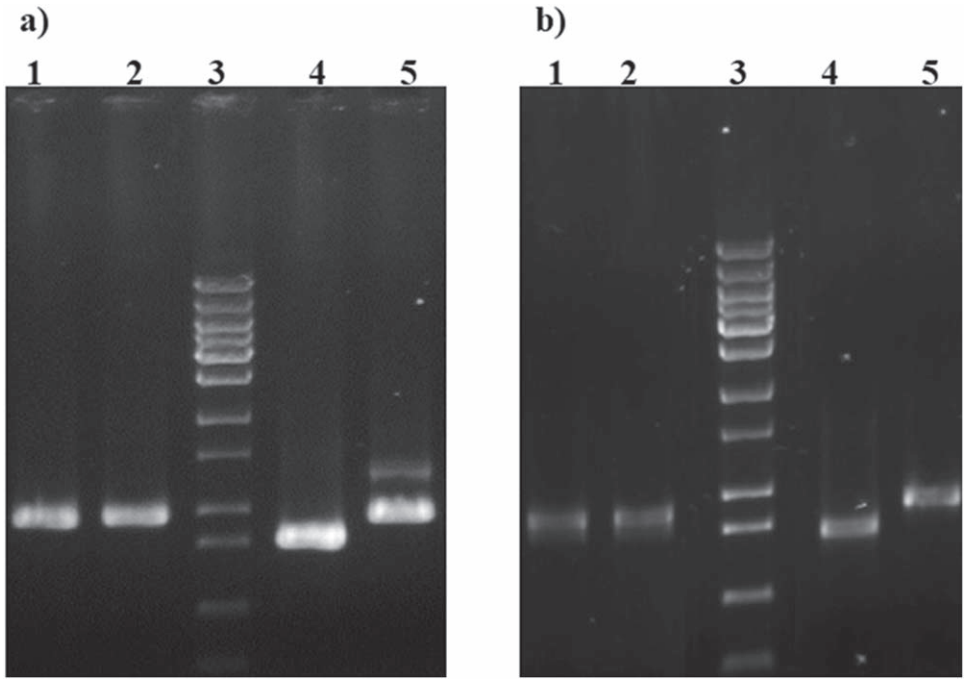

Figure 4. PCR confirmation of 5′ and 3′ junctions of *CNP*41 gene deletion in *C403*. (a) Deletion using *URA*3 selection marker: lane 1, 5′ landing with primers KC186/16 (775 bp); lane 2, 5′ junction with primers KC192/16 (811 bp); lane 3, 1 kb DNA Ladder; lane 4, 3′ landing with primers KC189/17 (755 bp); lane 5, 3′ junction with primers KC193/17 (901 bp). (b) Deletion using *LEU*2 selection marker: lane 1, 5′ landing with KC186/195 (775 bp); lane 2, 5′ junction with primers KC192/195 (811 bp); lane 3, 1 kb DNA Ladder; lane 4, 3′ Landing with primers KC189/206 (755 bp); lane 5, 3′ junction with primers KC193/206 (901 bp).

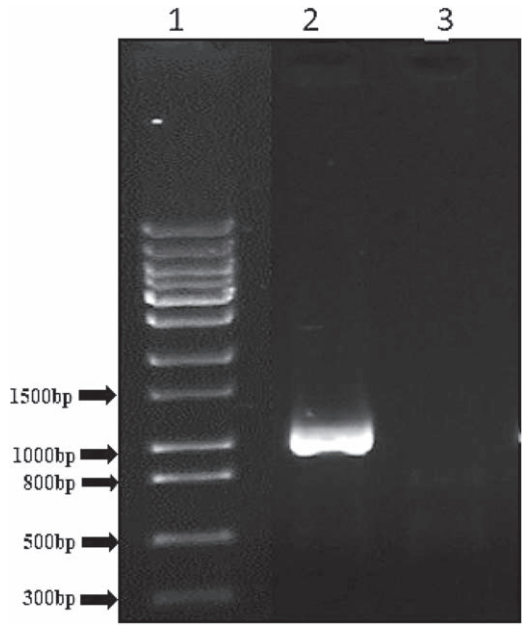

Figure 5. PCR verification of *CNP*41 gene null mutant. Lane 1, 1 kb DNA DNA ladder; lane 2, control PCR with CAF4-2 genomic DNA (1035 bp); lane 3, null mutant (C403), no PCR product amplified.

3.2. Biosynthesis of silver nanoparticles

Biosynthesis of silver nanoparticles using C86 strain of *C. albicans* was done by microwave assisted technique. The primary confirmation of the synthesised AgNPs was authenticated as the solution colour changed from pale yellow to brownish (see figure 6). Although some studies hypothesised that silver ions require NDPH dependent nitrate reductase enzyme for the reduction to AgNPs [28, 32], the exact mechanism of formation of AgNPs

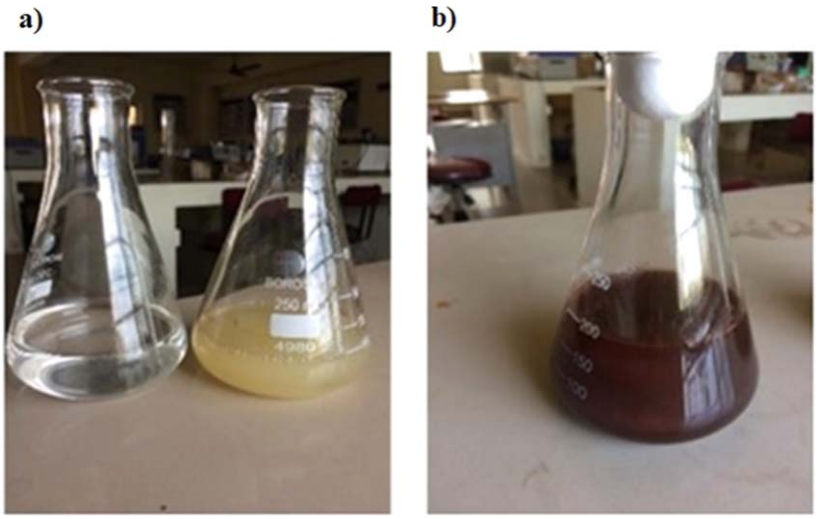

Figure 6. Synthesis of silver nanoparticles. (a) Transparent $AgNO_3$ solution (left) and pale yellow liquid culture (right) and (b) brown in colour synthesised AgNPs solution.

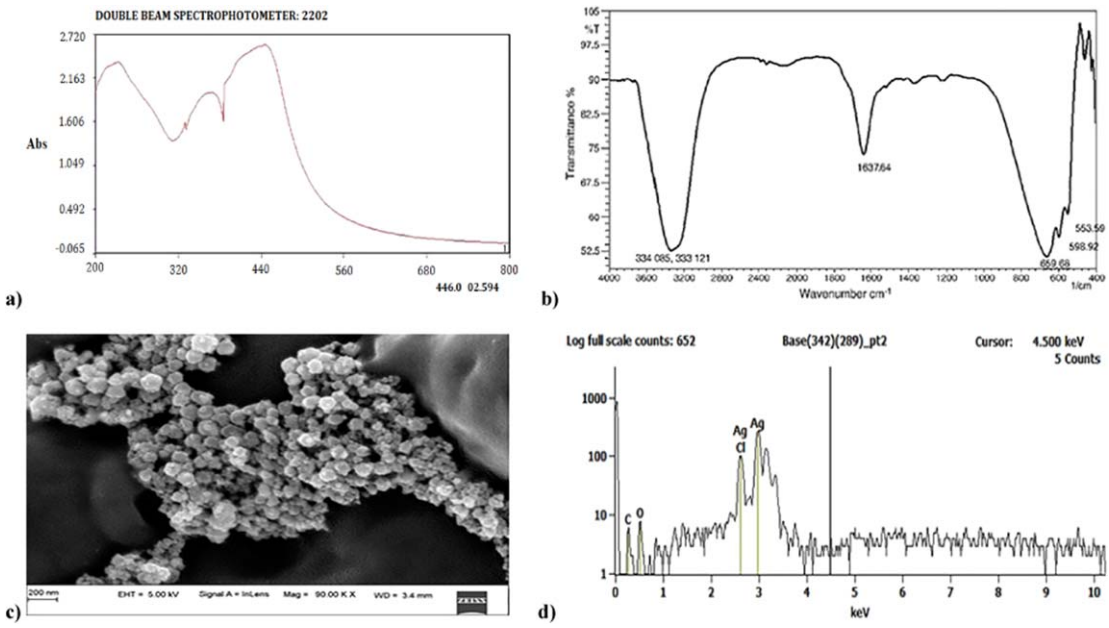

Figure 7. Characterization results of the biosynthesized AgNPs. (a) UV spectra of biosynthesized AgNPs. (b) FTIR spectra recorded from solid sample of synthesized AgNPs. (c) FESEM image of synthesized AgNPs. (d) EDX analysis plot of AgNPs from wild-type *Candida albicans* strain.

remains unanswered. One of the possible explanations for this study involving *C. albicans* is that the fungal cells secrete NDPH dependent nitrate reductase enzyme in their extracellular environment [29, 33].

3.2.1. Double beam UV spectrophotometer

Optical measurements for the primary detection of silver nanoparticles was done using UV-Visible spectrophotometer (Systronics 2202, India) and the range of wavelength was set between 200–800 nm. As depicted in figure 7(a), the maximum absorbance peak observed at wavelength 446 nm was within the AgNPs peak range [30]. This is in accordance with several studies that reported the highest absorbance peak between 400–480 nm [28, 29].

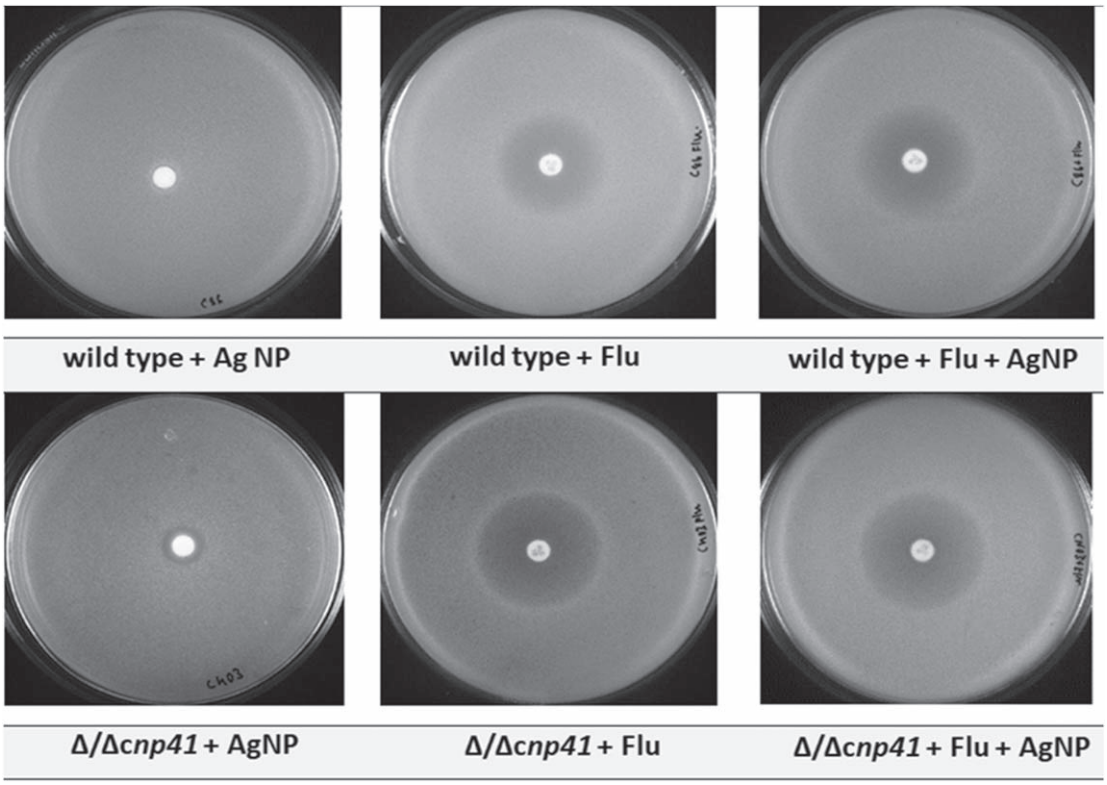

Figure 8. Zone of inhibition studies for analysis antifungal activity. Flu, fluconazole antifungal agent.

3.2.2. FTIR studies

For further characterisation of AgNPs, the solution was centrifuged to obtain pellets. As depicted in figure 7(b), FTIR solid sample analysis highlights the 6 bands involved, namely, 553.59, 598.92, 659.68, 1637.64, 3331.21 and 3340.85 cm^{-1}. This confirms the presence of AgNPs along with microbial enzymes. A similar study was carried out by Ukkund *et al* wherein the FTIR plots of biosynthesised AgNPs had peaks in the range of 4000–400 cm^{-1} [29]. This led to the understanding of the interactions between silver ions and enzymes in microbial solutions to stabilise the AgNPs. Figure 7(b) further highlights the presence of microbial proteins with the twisted shape of amide bonds. The peaks at 3340.85 (N–H stretch amide), 3331.21(stretching vibrations of primary amines), 1637.64 (C–O amides), 659.68 (C–N stretch amines), 553.59 (Ag–O) and 598.92 (C–Cl stretching) cm^{-1} verifying the presence of Ag nanoparticles. These peaks signify the involvement of N–H elongated vibrations, N–H bending vibrations and C=O elongating vibrations leading to microbial-silver nanoparticles aggregates [34]. The presence of the nitrate reductase enzymes on the surface of AgNPs was confirmed with the C–N and C–O–C stretching vibration [29]. The findings of Gole *et al* support this work with similar FTIR peaks describing the presence of AgNPs accompanied by enzymes and microbial proteins [35].

3.2.3. FESEM and EDX analysis

The topology and size of AgNPs were characterised by FESEM and as seen in figure 7(c), the AgNPs synthesised by using C86 strain of *C. albicans* was spherical in shape and its size ranged from 30–70 nm which is in accordance with the previous studies wherein 66 nm spherical shaped silver nanoparticles were reported [33]. Moreover, there results obtained are also comparable with those that incorporated other fungi like *penicillium spp.* [28, 29, 36]. Furthermore, EDX results are depicted in figure 7(d) and they are in accordance with the results observed for the AgNPs peaks exhibited in the FTIR studies. Lastly, EDX results confirm that 85.7% of AgNPs are present in the given sample and the results of this work is comparable with several studies reported in the literature [28–31, 34].

3.3. Antifungal activity of AgNPs

The antifungal activity of AgNPs was carried out by incorporating antifungal agent fluconazole as it shows fungistatic activity against most of the *candida* strains and helps in curing fungal infections [37]. Moreover, fluconazole belongs to azole class of antifungals and is more preferred due to its broad spectrum activity, high efficacy and low toxicity [6]. The zone of inhibition of AgNPs was studied against *Candida* strain C403 having both the copies of *CNP*41 gene deleted. The wild-type strain C86 has been used as a control. As seen in figure 8,

Table 4. Antifungal activity with respect to AgNPs and combination effect of AgNPs with respect to antifungal Fluconazole (Flu) on wild-type strain C86 and modified strain C403.

Candida albicans strain	Zone of inhibition with AgNP [mm]	Zone of inhibition with Flu (A) [mm]	Zone of inhibition with AgNP + Flu (B) [mm]	% Increase in Fold Area B-A/A*100
C86	0	27	29	7.4%
C403	10	29	32	10.3%

the C86 strain of *C. albicans* showed no zone on addition of AgNPs whereas the C403 strain showed a 10 mm zone around the 6 mm disk containing AgNPs. This finding is comparable with the works published on antifungal action on AgNPs by using ciprofloxacin [38], erythromycin [28] and fluconazole [35, 36, 38].

It has been shown earlier that metal and metal oxide nanoparticles have always stood apart for being an effective entities as antifungal agents [28, 29, 31]. Particularly, silver nanoparticles of triangle shaped and 75 nm sized were demonstrated effectively for presenting antifungal activity with Erythromycin against *penicillium spp*. [28], whereas spherical shaped silver nanoparticles of size 30–45 nm along with Erythromycin exhibited three-fold antifungal activity against *Fuzarium Oxysporum* [29]. Additionally, copper oxide nanoparticles of size 7 nm along with fluconazole were proven as effective antifungal agents against *C. albicans* [39]. These results are comparable with the current antifungal study wherein spherical biosynthesized silver nanoparticles of size 30–70 nm were tested positively against *Candida albicans*.

An enhanced microbial activity was seen as a promising result of having fluconazole antifungal agent with the synthesised AgNPs and supported by the works published by Balaji *et al* and Gajbhiye *et al* [36, 38]. Table 4 illustrates the increase in fold area activity. It was further observed that C403 strain had an increase in fold area by 10.3% when compared to the wild-type strain C86 with its fold area being 7.4%. This increase in the fold area can be attributed to the synergetic effect of the bonding reaction between fluconazole and AgNPs. Interestingly, AgNPs did not have any effect on wild-type C86 strain with its genes intact and the presence of AgNPs were insufficient to kill the strain. However, AgNPs had shown antifungal property on C403 strain having both the copies of *CNP*41 gene deleted. Thus, this study strongly suggests that the *CNP*41 gene could play a vital role in drug resistance in *C. albicans*.

4. Conclusion

The biosynthesis of silver nanoparticles (AgNPs) was carried out using wild-type *Candida albicans* strain C86 by adopting a novel approach. The formation of AgNPs was confirmed by several methods such as FTIR, UV spectrophotometer, EDX and FESEM. The results obtained from these analyses clearly indicated the formation of AgNPs. For testing the antifungal activity of this nanoparticles, a novel *Candida* strain C403 (*cnp*41Δ/*cnp*41Δ) has been generated by deleting both the copies of the *CNP*41 gene making the strain null mutant for this gene. The antifungal effect of AgNPs was studied on C403 (*cnp*41Δ/*cnp*41Δ) individually and in combination with antifungal drug fluconazole by the disk diffusion method whereas wild-type strain C86 serves as a control. An individual and enhanced combinational antifungal effect of AgNPs and fluconazole was observed on C403 strain with an increase in fold area of 10.3%. On the other hand, C86 strain remains unaffected for antifungal activity by AgNPs and a marginal increase was observed when in combination with fluconazole. This can be attributed to the synergetic effect of the bonding reaction between fluconazole and AgNPs. Thus, this study strongly suggests that *CNP*41 gene plays a critical role in drug resistance in *C. albicans*. Lastly, this work opens a plethora of opportunities to study the efficacy of AgNPs in various pathogenic fungi. Additionally, extensive experimental and clinical trials could be carried out to comprehend better use of AgNPs as a potential antimicrobial agent.

Acknowledgments

We thank Joachim Morschhäuser (Wurzburg, Germany) for providing us *Candida* plasmid. We thank also Judith Berman (University of Minnesoata, USA) and William Fonzi (University of California, USA) for *Candida* strain. We are thankful to Paike Jayadeva Bhat (IIT Bombay) for XL-1 strain and plasmid pUC19. We are thankful to National Institute of Technology Calicut to give Faculty Research Grant to Dr M Anaul Kabir.

ORCID iDs

Darshan Dhabalia https://orcid.org/0000-0002-8933-1396

Shareefraza J Ukkund https://orcid.org/0000-0002-5678-7426
Wasim Uddin https://orcid.org/0000-0001-9614-8461
M Anaul Kabir https://orcid.org/0000-0003-0042-7795

References

[1] Pellon A, Nasab S D S and Moyes D L 2020 New insights in *candida albicans* innate immunity at the mucosa: toxins, epithelium, metabolism, and beyond *Front. Cell. Infect. Biol.* **10** 81
[2] Ruben S *et al* 2020 Ahr1 and Tup1 contribute to the transcriptional control of virulence associated genes in *Candida albicans Mol. Biol. Physiol.* **11** e00206–20
[3] Robles-Martíne M *et al* 2020 Mentha piperita as a natural support for silver nanoparticles: a new anti *Candida albicans* treatment *Colloid Interface Sci. Commun.* **35** 100253
[4] Kabir M A, Hussain M A and Ahmad Z 2012 *Candida albicans*: a model organism for studying fungal pathogens *ISRN Microbiology* **2012** 538694
[5] Padmavathi A R *et al* 2020 Impediment to growth and yeast-to-hyphae transition in *Candida albicans* by copper oxide nanoparticles *Biofouling* **36** 56–72
[6] Zhang M *et al* 2020 Antifungal activity of ribavirin used alone or in combination with fluconazole against *Candida albicans* is mediated by reduced virulence *Int. J. Antimicrob. Agents* **55** 105804
[7] de Oliveira Santos G C *et al* 2018 *Candida* infections and therapeutic strategies: mechanisms of action for traditional and alternative agents *Front. in Microbiol.* **9** 1351
[8] Amini S M and Akbari A 2019 Metal nanoparticles synthesis through natural phenolic acids *IET Nanobiotechnol.* **13** 771–7
[9] Shuaib U *et al* 2020 Plasma-liquid synthesis of silver nanoparticles and their antibacterial and antifungal applications *Mater. Res. Express* **7** 035015
[10] Dung T T N, Nam V N and Nhan T T 2020 Silver nanoparticles as potential antiviral agents against African swine fever virus *Mater. Res. Express* **6** 1250g9
[11] Pereira T M, Polez V L P, Sousa M H and Silva L P 2020 Modulating physical, chemical and biological properties of silver nanoparticles obtained by green synthesis using different parts of the tree Handroanthus heptaphyllus (Vell.) Mattos *Colloid Interface Sci. Commun.* **34** 100224
[12] Mehrizi M K 2020 Application of plant-based natural product to synthesize nanomaterial *Nanomaterials in Biofuels Research: Clean Energy Production Technologies* 1st edn, ed M Srivastava *et al* (Singapore: Springer Nature) pp 53–74
[13] Vijayan S *et al* 2020 Antifungal efficacy of Chitosan-stabilized biogenic silver nanoparticles against pathogenic Candida spp. Isolated from Human *BioNanoSci.* **10** 974–82
[14] Gaur M, Choudhury D and Prasad R 2005 Complete inventory of ABC proteins in human pathogenic yeast, *Candida albicans J. Mol. Microbiol. Biotechnol.* **9** 3–15
[15] Fonzi W A and Irwin M Y 1993 Isogenic strain construction and gene mapping in *Candida albicans Genetics* **134** 717–28
[16] Reddy P K *et al* 2020 CSU57 encodes a novel repressor of sorbose utilization in opportunistic human fungal pathogen *Candida albicans Yeast* **37** YEA3537
[17] Morschhäuser J, Michel S and Staib P 1999 Sequential gene disruption in *Candida albicans* by FLP-mediated site-specific recombination *Mol. Microbiol.* **32** 547–56
[18] Gough J A, Murray N E and Brenner S 1983 Sequence diversity among related genes for recognition of specific targets in DNA molecules *J. Mol. Biol.* **166** 1–19
[19] Sherman F 1990 Getting started with the yeast *Guide to Yeast Genetics and Molecular Biology* ed J Abelson and M Simon 1st edn. (New York: Academic) pp 3–41
[20] Perepnikhatka V *et al* 1999 Specific chromosome alterations in fluconazole-resistant mutants of *Candida albicans J. Bacteriol.* **181** 4041–9
[21] Saiki R K *et al* 1988 Primer-directed enzymatic amplification of DNA with a thermostable DNA polymerase *Science* **239** 487–91
[22] Sambrook J F and Russell D W 2001 *Molecular Cloning: A Laboratory Manual* (New York: Cold Spring Harbor Laboratory Press)
[23] Birnboim H C and Doly J 1979 A rapid alkaline extraction procedure for screening recombinant plasmid DNA *Nucleic Acids Res.* **7** 1513–23
[24] Cohen S N, Chang A C Y and Hsu L 1972 Non-chromosomal antibiotic resistance in bacteria by genetic transformation of *Escherichia coli* by R-factor DNA *Proc. Natl Acad. Sci. USA* **69** 2110–4
[25] Hinnen A, Hicks J B and Fink G R 1978 Transformation of yeast *Proc. Natl Acad. Sci. USA* **75** 1929–33
[26] Kabir M A and Rustchenko E 2005 Determination of gaps by contig alignment with telomere-mediated chromosomal fragmentation in *Candida albicans Gene* **345** 279–87
[27] Yanisch-Perron C, Vieira J and Messing J 1985 Improved M13 phage cloning vectors and host strains: nucleotide sequences of the M13mp18 and pUC19 vectors *Gene* **33** 103–19
[28] Ukkund S J, Rani M N, Anand S and Rangappa D 2017 Synthesis and characterization of silver nanoparticles from *Penicillium Spp Mater. Today: Proc.* **4** 11923–32
[29] Ukkund S J *et al* 2019 Synthesis and characterization of silver nanoparticles from *Fuzarium Oxysporum* and Investigation of their Antibacterial activity *Mater. Today: Proc.* **9** 506–14
[30] Clinical and Laboratory Standard Institute 2018 *Performance Standards of Antimicrobial disk Susceptibility Tests; Approved Standard—13th ed. CLSI Document M02* (Wayne, PA, USA: Clinical and Laboratory Standards Institute)
[31] Nishanthi S, Malathi S, Paul S J and Palani P 2019 Green synthesis and characterization of bioinspired silver, gold and platinum nanoparticles and evaluation of their synergistic antibacterial activity after combining with different classes of antibiotics *J. Mater. Sci. Eng* C **96** 693–707
[32] Hietzschold S, Walter A, Davis C, Taylor A A and Sepunaru L 2019 Does nitrate reductase play a role in silver nanoparticle synthesis? Evidence for NADPH as the sole reducing agent *ACS Sustainable Chem. Eng.* **7** 8070–6
[33] Ingle A, Gade A, Pierrat S, Sonnichsen C and Rai M 2008 Mycosynthesis of silver nanoparticles using the fungus *Fusarium acuminatum* and its activity against some human pathogenic bacteria *Curr. Nanosci.* **4** 141–4
[34] Bhat M A, Nayak B K and Nanda A 2015 Evaluation of bactericidal activity of biologically synthesised silver nanoparticles from *Candida albicans* in combination with Ciprofloxacin *Mater Today:Proc.* **2** 4395–401
[35] Gole A *et al* 2001 Pepsin-gold colloid conjugates: preparation, characterization, and enzymatic activity *Langmuir* **17** 1674–9

[36] Gajbhiye M *et al* 2009 Fungus mediated synthesis of silver nanoparticles and their activity against pathogenic fungi in combination with Fluconazole *Nanomed. Nanotechnol. Biol. Med.* **5** 382–6
[37] Kirkpatrick W R *et al* 1998 Fluconazole disk diffusion susceptibility testing of *Candida* species *J. Clin. Microbiol.* **36** 3429–32
[38] Balaji D S *et al* 2009 Extracellular biosynthesis of functionalized silver nanoparticles by strains of *Clostridium cladosporiodes* fungus *Colloids Surf.* B **68** 88–92
[39] Weitz I S *et al* 2015 Combination of CuO nanoparticles and fluconazole: preparation, characterization, and antifungal activity against *Candida albicans J. Nanopart. Res.* **17** 342